

# Towards a Hybrid Agent-based Model for Mosquito Borne Disease

S. M. Mniszewski<sup>1</sup>, C. A. Manore<sup>2</sup>, C. Bryan<sup>3</sup>, S. Y. Del Valle<sup>1</sup>, and D. Roberts<sup>4</sup>

<sup>1</sup>Los Alamos National Laboratory, Los Alamos, NM 87545

<sup>2</sup>Tulane University, New Orleans, LA 70118

<sup>3</sup>University of California, Davis, CA 95616

<sup>4</sup>Research Triangle Institute, Durham, NC 27709

*smm@lanl.gov, cmanore@tulane.edu, cjbryan@ucdavis.edu, sdelvall@lanl.gov, droberts@rti.org*

**Keywords:** agent-based modeling, discrete event simulation, mathematical modeling, epidemic modeling, mosquito borne disease modeling

## Abstract

Agent-based models (ABM) are used to simulate the spread of infectious disease through a population. Detailed human movement, demography, realistic business location networks, and in-host disease progression are available in existing ABMs, such as the Epidemic Simulation System (EpiSimS). These capabilities make possible the exploration of pharmaceutical and non-pharmaceutical mitigation strategies used to inform the public health community. There is a similar need for the spread of mosquito borne pathogens due to the re-emergence of diseases such as chikungunya and dengue fever. A network-patch model for mosquito dynamics has been coupled with EpiSimS. Mosquitoes are represented as a “patch” or “cloud” associated with a location. Each patch has an ordinary differential equation (ODE) mosquito dynamics model and mosquito related parameters relevant to the location characteristics. Activities at each location can have different levels of potential exposure to mosquitoes based on whether they are inside, outside, or somewhere in-between. As a proof of concept, the hybrid network-patch model is used to simulate the spread of chikungunya through Washington, DC. Results are shown for a base case, followed by varying the probability of transmission, mosquito count, and activity exposure. We use visualization to understand the pattern of disease spread.

## 1. INTRODUCTION

Mosquito-borne pathogens pose a significant threat to human health around the world due to globalization, which can increase the chances of introduction of mosquito-borne pathogens into naive regions. For example, West Nile virus, previously absent from the Americas, was introduced to New York in 1999 and subsequently spread across the contiguous United States in less than 5 years. Dengue has caused increasing concern due to re-emergence in areas where it had been absent for years [14] and the risk may increase due to climate change [3]. Recently, chikungunya virus re-emerged in

Asia and caused outbreaks in Italy and several Indian Ocean islands [2, 34].

The primary vectors for both chikungunya and dengue are *Aedes aegypti* and *Aedes albopictus* mosquitoes, which generate acute infections in humans. Local cases of dengue have been confirmed in southern Texas and southern Florida, increasing the concern about continued emergence in the United States. Chikungunya has been absent from North America, but a small outbreak is ongoing in the Caribbean, providing fear of increased risk for introduction on the continent [18]. Since the primary vectors of chikungunya are present in much of South, Central, and southern North America, risk of outbreaks if introduced, could be high.

There is a growing need to understand the critical parameters in the transmission and persistence of these diseases, to quantify the risk of spread, and to develop effective strategies for prevention and control. There have been several efforts to model chikungunya since the recent outbreaks using continuous non-spatial ordinary differential equation models (e.g. [4, 27]). Dumont *et al.* 2008 and 2010 [10, 11] modeled chikungunya spread for the recent R union Island strain, including control measures and increased transmission in *A. albopictus*. Moulay *et al.* 2011 and 2012 [24, 25] and Yakob & Clements [38] modeled the first outbreak of chikungunya on R union Island. These modeling efforts provided important analysis and parameter estimates for chikungunya. However, models that incorporate spatial and temporal heterogeneity in mosquito ecology, as well as human behavior and movement are needed. Human movement and spatio-temporal heterogeneity have been shown to play a significant role in risk and control of mosquito-borne pathogens [1, 7, 29, 32].

Adams and Kapan, 2009, [1] modeled spatial mosquito-borne disease on a network where each network node corresponded to exactly one patch and where the mosquito populations did not explicitly depend on weather or landscape. Others have used disaggregated spatial data for human and mosquito populations to estimate risk of dengue in Oahu, providing risk of human exposure to mosquito bites at a particular time [36]. Chao *et al.* [6] developed a model for individual humans and individual mosquitoes for semi-rural villages in

Thailand to explore the effects of vaccine on dengue transmission. Perkins et al. [26] explored the idea of different habitat patches for various mosquito life cycle stages (blood seeking, resting, oviposition) with movement of humans based on proportion of time spent in each of the patches that are related to mosquito behavior. We expand on and extend these models by considering mosquito habitat patches within which mosquito dynamics are aggregated where patch mosquito parameters will be determined by landscape, land use, weather, socio-economic factors, and current data about mosquito species and density.

Here, we describe the process of adapting a detailed, large-scale individual based model for human behavior and movement to model mosquito-borne disease using the network-patch method described in [19]. Rather than attempt to model each mosquito individually as in [5, 41], we overlay a region through which humans are moving with mosquito habitat patches that determine the risk of a human being bitten while in the area. This will provide important information about risk of outbreaks and control strategies for mosquito-borne disease, particularly in urban environments.

## 2. METHODS

### 2.1. Agent-based Population Dynamics

EpiSimS [22, 23, 33] is an agent-based model that combines three different sets of information to simulate disease spread within a geographic area: population (e.g., demographics), locations (e.g., buildings, rooms, and mixing places), and movement of individuals between locations (e.g., activity schedules). We simulated the spread of a chikungunya outbreak in Washington, DC with a synthetic population constructed to statistically match the 2000 population demographics at the census tract level. The synthetic population consists of 0.5 million individuals living in 0.25 million households, with an additional 40 thousand locations representing actual schools, businesses, shops, or social recreation addresses. The synthetic population of Washington, DC represents only individuals reported as household residents in the 2000 U.S. Census. The simulation ignores visiting tourists and does not explicitly treat travelers in hotels and airports.

We use the National Household Transportation Survey (NHTS) [35] to assign a schedule of activities to each individual in the simulation. Each individual's schedule specifies a starting and ending time, type, and location of each assigned activity. Information about the time, duration, and location of activities is obtained from the NHTS. The five types of activities are: home, work, shopping, social recreation, school, and other. The time, duration, and location of activities determines which individuals are together at the same location at the same time. This is relevant in the spread of infectious disease between humans and similarly for vector borne disease between humans and mosquitoes.

Each location is geographically-located using the Dun & Bradstreet commercial database and is subdivided into buildings based on the activities available at that location. Each building is further subdivided into rooms or mixing places. Examples include a classroom in a school, an office or meeting room at work, a shop in a shopping mall, and a soccer field for social recreation. Typical room sizes can be specified. The mean workgroup size varies by standard industry classification (SIC) code. We estimated the mean workgroup size by SIC from two data sources: a study on employment density [39] and a study on commercial building usage from the Department of Energy [21]. The mean workgroup size ranges from 3.1 people for transportation workers to 25.4 for health service workers. The average over all SIC's for work is 15.3 workers per workgroup. For the analyses presented here, the average mixing group sizes are: 8.5 people at a school, 4.4 at a shop, and 3.5 at a social recreation venue. While mixing group size is the elemental unit in human-to-human transmission of disease, transmission between humans and mosquitoes is handled at the location level with variations of exposure level by activity.

### 2.2. Mosquito Borne Disease Progression

Chikungunya is an arbovirus first identified in 1953 [30]. As with dengue, chikungunya has a relatively low death rate, but often causes disease with symptoms similar to dengue fever accentuated by severe arthritis-type pain [30]. Once infected, immunity is thought to last for life and there is thought to be cross-immunity between strains. Mitigation strategies for chikungunya are similar to those used for dengue, namely mosquito control.

Diseases such as influenza are passed from human-to-human during close proximity through contact, sneezing, coughing, or via fomites. In contrast, mosquito borne diseases are transmitted from human-to-mosquito and mosquito-to-human.

When a non-infected, or susceptible ( $S_v$ ), female mosquito bites a human infected with chikungunya, the mosquito has a positive probability of acquiring the pathogen. If the mosquito is infected, the virus must reproduce in the mosquito and make its way to the mosquito's salivary glands. The time that this process takes is called the extrinsic incubation period and is often on the same order as a mosquito's average lifespan. Mosquitoes in this stage are denoted by  $E_v$  in the model. Once the virus reaches the salivary glands of a female mosquito, the infectious mosquito ( $I_v$ ) can transmit the virus to a susceptible human, thus completing the cycle. We assume that mosquitoes never recover from the pathogen but die infectious. Note that male mosquitoes do not require blood meals, so we only consider female mosquitoes in the model. Once a human is infected, the virus replicates in the human during an incubation period, after which the human

is infectious to mosquitoes (and likely symptomatic). We assume that once a human recovers from the virus, he/she is immune for life.

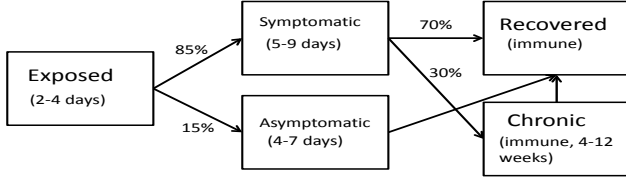


Figure 1: Disease progression states of chikungunya in humans. The arrows represent movement of individuals from one stage to the next.

In EpiSimS, in-host (human) disease progression of chikungunya is modeled as a markov chain consisting of five main epidemiological stages: exposed (not infectious), symptomatic (infectious), asymptomatic (infectious), chronic, and recovered (see Figure 1). Once exposed, a person incubates for 2 to 4 days, before transitioning to the symptomatic or asymptomatic stages, where 86% become symptomatic. A person is infectious to mosquitoes for 5-9 days when symptomatic and 4-7 days when asymptomatic. 70% transition to the recovered stage, while 30% become chronic for 4-12 weeks before recovering. All age groups progress similarly.

### 2.3. Ordinary Differential Equations for Patches of Mosquitoes

Each mosquito patch is characterized by the scalar parameters specific to that patch. Patches are chosen so that the mosquitoes can be well approximated by a mean-field, homogeneous mixing model using differential or discrete equations. There is a rich history of modeling mosquito populations in the context of mosquito-borne diseases such as dengue and chikungunya using simple ordinary differential equations [4, 10, 11, 13, 24, 27, 37, 38]. Our mosquito dynamics model for a patch (see Figure 2) is described as a system of ODEs as follows:

$$\frac{dS_v}{dt} = h_v(N_v, t) - \lambda_v(t)S_v - \mu_v S_v \quad (1)$$

$$\frac{dE_v}{dt} = \lambda_v(t)S_v - \nu_v E_v - \mu_v E_v \quad (2)$$

$$\frac{dI_v}{dt} = \nu_v E_v - \mu_v I_v. \quad (3)$$

The total number of adult female mosquitoes,  $N_v = S_v + E_v + I_v$ , includes all susceptible, exposed incubating, and infectious mosquitoes in the patch. The average force of infection to mosquitoes,  $\lambda_v(t)$  (rate of infection for each mosquito at time  $t$ ), in the patch is defined as the product of the average number of bites per mosquito (determined by  $\sigma_h$  and  $\sigma_v$ ), the

probability that a bite is on an infectious human ( $I_h(t)/N_h(t)$ ), and the probability of transmission per bite ( $\beta_{vh}$ ). This rate varies with time as the proportion of infectious humans occupying the patch varies and is updated at each time step by coupling with the human movement model. A full description of the mosquito model comes from [8, 20] and can be found in [19].

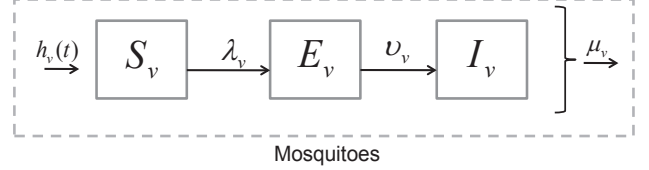


Figure 2: Susceptible ( $S_v$ ), exposed incubating ( $E_v$ ), and infectious ( $I_v$ ) mosquito ODE model.

The adult female mosquito per-capita emergence function,  $h_v(N_v, t)$ , is  $h_v(N_v, t) = \left(\psi_v - \frac{r_v N_v}{K_v}\right) N_v$  where  $\psi_v$  is the natural per-capita emergence rate of female mosquitoes in the absence of density dependence,  $\mu_v$  is the natural mosquito death rate, and  $r_v = \psi_v - \mu_v$  is the mosquito population growth rate. The total mosquito population in each patch is modeled by:

$$\frac{dN_v}{dt} = r_v \left(1 - \frac{N_v}{K_v}\right) N_v. \quad (4)$$

This model can incorporate vector control measures explicitly to the different life stages of the mosquito. Some of the more important time dependent parameter variations are seasonal mosquito recruitment rate, seasonal biting rate, seasonal mortality rate, and a temperature-dependent seasonal extrinsic incubation period. This mosquito ODE model produces a risk of transmission for humans who are bitten.

### 2.4. Network Patch Model

Extending the EpiSimS framework, we have added the patch concept and disease transmission between humans and mosquitoes. A patch is associated with each location. A patch represents a “patch” or “cloud” of mosquitoes, not individual mosquitoes. Each patch has an associated mosquito ODE model. Patch parameters can vary between patches and consist of those required for the ODE model (see Table 1), such as number of mosquitoes, probability of transmission from human to mosquito and from mosquito to human. Additionally, each activity at a location has an associated activity exposure dependent on being indoors, outdoors, or somewhere in-between, ranging from 0.0, for no exposure, to 1.0, for full exposure.

The population moves through their scheduled activities between locations. Disease transmission between humans and mosquitoes for our Washington, DC example is checked on

Table 1: Mosquito dynamics parameters for patch ODE model (first 8 parameters) and those used when coupling the human model with the mosquito patch model (last 4 parameters).

Name	Description
$\Psi_v$	Per capita birth rate of female mosquitoes
$\sigma_v$	Max number of successful mosquito bites per day
$\beta_{vh}$	Prob. of transmission from human to mosquito
$v_v$	Per capita rate of progression of mosquitoes from exposed/incubating to infectious
$\mu_v$	Per capita death rate of adult female mosquitoes
$r_v$	Per capita intrinsic rate of growth for mosquitoes
$K_v$	Number of mosquitoes in patch
$\sigma_h$	Max number of bites received by humans per day
$N_h$	Total number of humans available for biting
$I_h$	Total number of infectious humans available for biting
$\beta_{hv}$	Prob. of transmission from mosquito to human
$\delta_h$	Time step converted to fraction of day

an hourly basis. Total number of people and total infected (infectious) are collected within a patch as a weighted sum based on the activity exposure. These values and the time step serve as input to the mosquito ODE model. A susceptible patch can become infected if infectious people are present. A biting risk is returned from the ODE model and is used along with the activity exposure to randomly decide if a susceptible person becomes exposed.

A fourth order Runge Kutta method [28] is used to approximate the ODE system. The number of susceptible mosquitoes, exposed/incubating mosquitoes, and infectious mosquitoes are updated every time the disease transmission is run.

The biting risk is tracked per patch. Events and infection records are recorded whenever a person or patch become infected. These are later post-processed for analysis and visualization.

## 2.5. Visualization of Disease Spread

To help analyze the spread of infection, we implement a geospatial visualization which shows time-dependent and time-aggregated infection data. Geospatial visual analytics have been shown to be an effective method for understanding epidemic spread, hotspotting, and diffusion [9, 17, 40]; it is therefore a natural approach for analyzing the spatiotemporal spread of chikungunya. The view system is implemented using the D3 javascript library [12] and Leaflet mapping library [16], and overlays two selectable layers of infection data on a 2-D map of Washington, DC. The initial layer is a set of points showing infection events. An infection event oc-

curs when chikungunya is transmitted between a person and mosquito.

The second data layer is a kernel density estimation (KDE) of infected patches or infected people for a given day. KDE is a non-parametric way to take a set of sample points containing some feature and estimating the statistical density of that feature in a spatial neighborhood, based on a chosen kernel function [31]. In calculating a day's infected population density, for each infected person we aggregate all the locations they visit with the fraction of that day's time that person spends at each location. The set of times and locations is summed together over the day's 24 hour period. If infected patches are selected to be shown instead of people, a chosen patch feature from Table 1 such as  $\beta_{vh}$  or  $K_v$  is the feature that the KDE calculation is performed on. For our analysis, we found the number of mosquitos in a patch ( $K_v$ ) the most helpful indicator of patch influence.

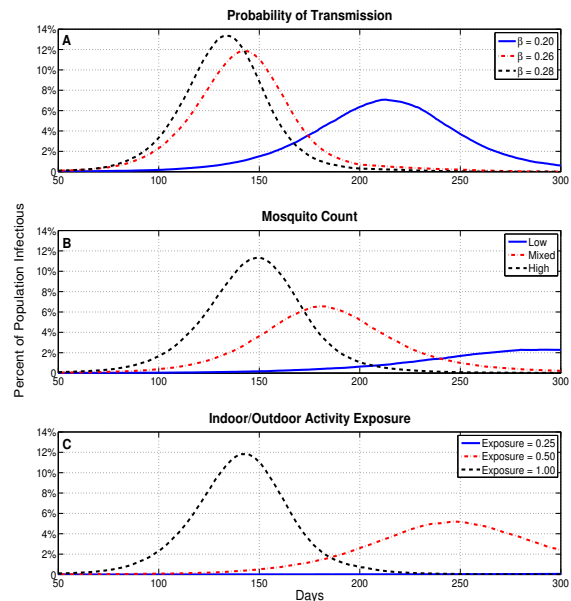


Figure 3: Plots showing percent of population infectious over time for A) varying the probability of transmission (0.20, 0.26, 0.28), B) varying the mosquito count (low, mixed, high), and C) varying the indoor/outdoor activity exposure (0.35, 0.50, 1.00).

## 3. RESULTS

Using simulation we varied the important mosquito ODE model parameters to understand their effect on the spread of disease. We used the Washington, DC area and synthetic population due to its small size and as a proof of concept. This is

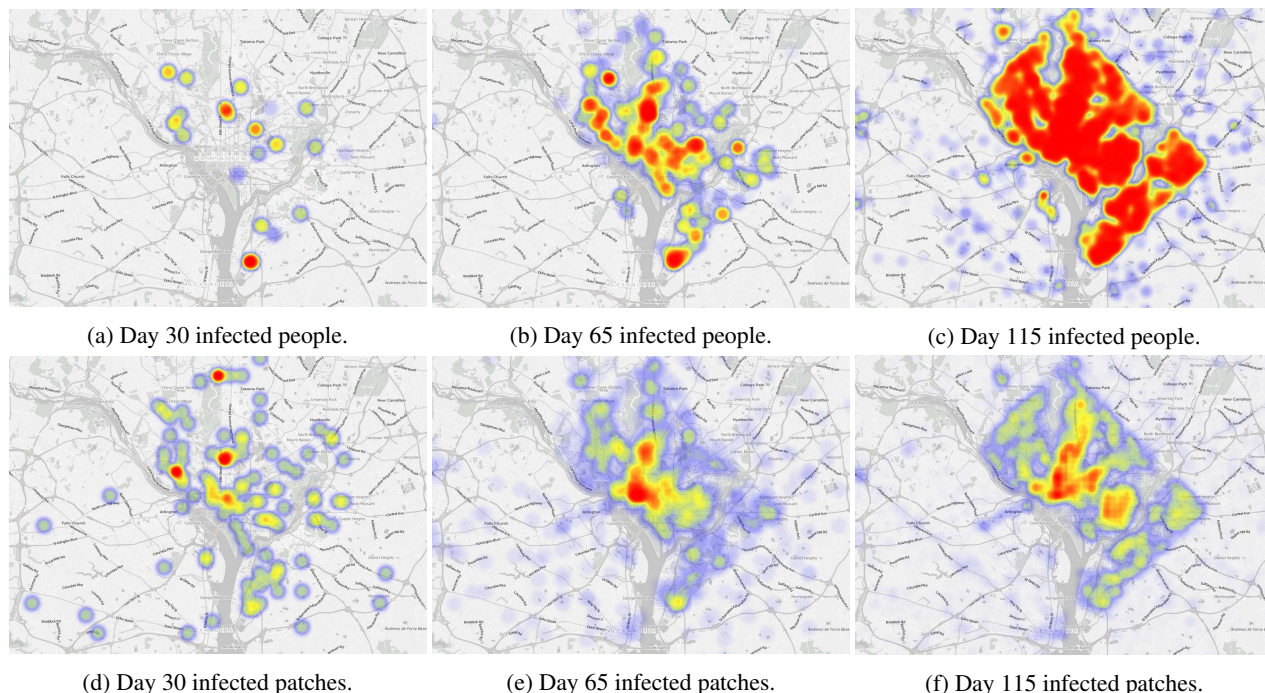


Figure 4: Snapshots of the base case at three days representing the early, middle, and incidence peak of the epidemic. The top row shows the densities of infected people, while the bottom row shows the densities of infected patches.

not a city that is typically associated with major outbreaks of mosquito borne disease, though it is representative of many urban communities across the globe in its lack of mosquito control programs [15]. Our experiments are all based on hypothetical scenarios.

The Washington, DC population consists of 0.5 M people, 0.25 M homes, and 40 K business locations. All experiments started with 21 random index cases as infected humans. These people go on to infect mosquito patches, which in turn infect more people, etc. The parameters that we explored in these experiments are relevant to tuning a base case scenario and to understand how they affect outcomes.

We considered the probability of transmission from humans to mosquitoes and from mosquitoes to humans ( $\beta_{hv}$  and  $\beta_{vh}$ ), mosquito count ( $K_v$ ), and activity exposure. These parameters can be set on a per patch basis. In our experiments the probability of transmission between humans and mosquitoes ( $\beta_{hv}$  and  $\beta_{vh}$ ) is the same across all patches (and locations) representing one type of mosquito and a common human response. The value is the same for both and can be 0.20-0.33. The mosquito count ( $K_v$ ) is allowed to vary across patches. It is assumed to be 20,000 around a swamp, less in other places. However, note that one needs information about land use to predict this accurately. Activity exposure represents the level of potential exposure whether inside (0.0), outside (1.0), or somewhere in-between (0.6). This parameter

takes on values 0.0-1.0. One value for each activity (ex. home, work, shopping, social recreation, school, and other) taking place in a patch (based on location). Closed work buildings with air conditioning will be set to 0.0, while homes with torn screens and open porches may be set to 0.6.

In all cases one parameter is varied, while the others are held constant. We performed 3 sets of experiments as follows. The first varied the probability of transmission as 0.20, 0.26, and 0.28. The mosquito count was 5,000 and the activity exposure was 1.0 for all patches. The second varied the mosquito count with a fixed probability of transmission of 0.26 and activity exposure of 1.0 for all patches. Different numbers of mosquitoes were randomly assigned to each patch. Scenarios included low counts (0, 100, 500, 1,000), high counts (2,000, 3,000, 4,000, 5,000), and mixed (0, 100, 500, 1,000, 2,000, 3,000, 4,000, 5,000). The third experiment varied activity exposure with probability of transmission 0.26 and mosquito count 5,000 for all patches. Activity exposure scenarios included very low (0.1), low (0.25), medium (0.5), and high (1.0). The activity exposure was the same for all activities in a patch.

### 3.1. Human-Mosquito Probability of Transmission

Our goal was to tune the probability of transmission between humans and mosquitoes ( $\beta_{hv}$  and  $\beta_{vh}$ ) such that preva-

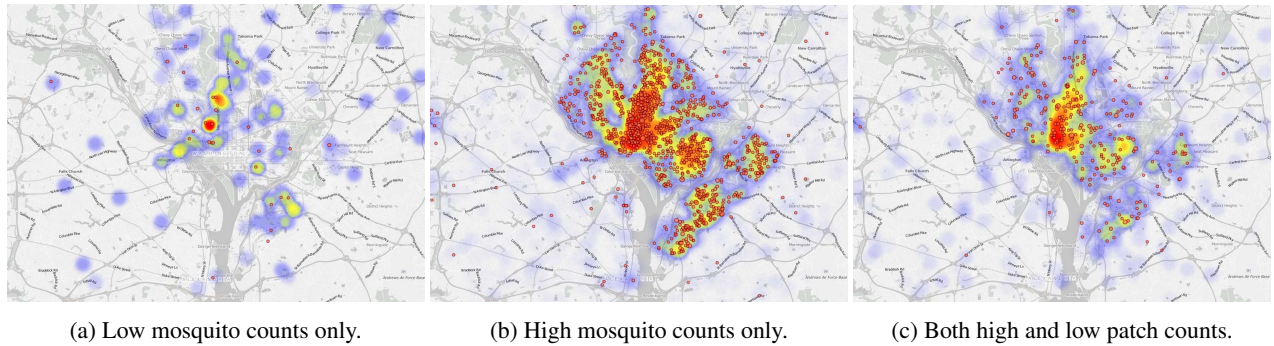


Figure 5: Showing all infection points over mosquito density at day 100 when varying the mosquito counts in patches. (a) Low mosquito counts hinder the growth rate, although it still spreads out geospatially. (b) More mosquitos equate to higher and faster transmission rates, and thus a more quickly diffusing disease spread. (c) Varying the amount of mosquitos in patches shows a growth and distribution rate between the two extremes.

lence or infectious humans peaked around day 140-150 at 10-12% of the population spread between day 100 and 200. This is similar to the experiment results shown in Figure 3 of Manore et al. [19] where humans have high movement. As seen in Figure 3A, a lower value of 0.20 produces slow moving transmission, with a large spread, and a low peak. A higher value, such as 0.26 or 0.28, results in faster transmission, a higher peak, and a narrower spread. The value of 0.26 produced a prevalence curve most similar to our criteria and becomes our base case.

When analyzing the base case in more detail we also consider the incidence or new infections per day. We plot the densities of infected people and infected patches to show how the epidemic diffuses over time. Starting with a small seed of infected people who travel around the area, patches become infected, and in turn infect more people. Infected people travel around infecting patches and then recover, but patches stay infected, leading to a saturated spatial dispersion of infected patches. We plot three timesteps of the base case: an early stage, middle stage, and peak incidence of the epidemic, for days 30, 65, and 115, as shown in Figure 4.

At day 30, we see a sparse distribution of both currently infected people and infected patches. By day 65, the number of currently infected people are forming density clusters in the Washington, DC metro area. Hotspots of infected patches also appear here, although the diffusion of patches is more evenly spread around the central city and sparsely spread around the map's edges. By day 115, the city has a heavy density of both infected people and patches, though patches are still more evenly spread over the entire map. The pattern of infection spread we observe is thus: the infection jumps around patches in its spread, but only heavily visited locales such as downtown Washington, DC grow in infection density over time. Less populated areas see only sporadic infection.

### 3.2. Mosquito Count in Patch-Locations

Starting with the base case, we vary the mosquito count per patch ( $K_v$ ) as low counts (0-1,000), high counts (2,000-5,000), and mixed (0-5,000). Mosquito counts are assigned randomly to patches. Figure 3B shows that lower counts slow transmission and reduce the peak, while higher counts increase the transmission rate and peak. The high counts are similar to the base case.

To show how varying the counts of mosquitos in patches affects transmission and diffusion, we plot the infection rate of people over time when mosquito counts in patches are low, high, and mixed (Figure 5) for the first 100 days of the epidemic. High counts of mosquitos lead to the fastest transmission and highest peaks, while low counts give the opposite effect. Mixed mosquito counts run a middle ground between transmission rate and infection peak. To visualize the rate of spread and infection, we map the three different mosquito counts at day 100. For each location where an infection occurred, we mark a point, colored darker according to how long in the past the initial infection at that location happened. Underneath this point layer, we apply a patch density layer, based on the mosquito count value ( $K_v$ ). This layering shows the distribution of infectious mosquitos and how it correlates to infecting humans over the course of each simulation's first 100 days.

Figure 5a only contains low mosquito counts in patches, and has relatively few infection points and patches. There is hotspotting in the middle of the map, but patches are sparsely distributed around this clustering. Figure 5b has high mosquito counts in all its patches, and shows a large infection area in the central part of the map. The surrounding area has an even distribution of infected patches, but the Washington, DC metro area is still where most infections occur. The last figure, 5c, has varying counts of mosquitos in its patches. It shows hotspotting in the central part of the map, with a

ring of less dense infected patches around that, and sparser infected patches around the edges of the map. For all three maps, most humans become infected only in highly dense areas of infectious mosquitos, corresponding to central Washington DC. However, the total number of infected people and patches varies greatly depending on the counts of mosquitos in the patches themselves.

### 3.3. Activity Exposure

Starting with the base case, we vary the activity exposure. Activity exposure is the same value for all activities at all locations. A very low activity exposure of 0.1 results in little transmission and is not shown. In Figure 3C low exposure (0.25) shows less than 1% prevalence over time. Medium exposure (0.50) produces slowed transmission and a reduced peak, compared to the high exposure (1.0) in the base case.

## 4. DISCUSSION

We have a working hybrid network-patch EpiSimS ABM coupled with mosquito ODE dynamics. Proof of concept experiments demonstrated the effect of varying ODE parameters, such as the probability of transmission, mosquito count, and activity exposure. High values for the probability of transmission can speed transmission, producing a higher prevalence peak and narrower spread. Lower mosquito counts per patch slow transmission and activity exposure can dramatically reduce exposure even at a medium (0.5) level.

There is much heterogeneity over any geographical area. Mosquito counts per patch (or location) and activity exposure can be estimated based on knowledge about the area. The probability of transmission can then be tuned for a faster or slower rate of transmission to match prevalence for a known outbreak.

Through visualization we were able to capture the pattern of disease spread. In our example, infection sites begin randomly based on frequently visited locations, large mosquito counts, and increased activity exposure. These are seen to grow into larger density areas over time.

Future plans include validation using historical outbreak data and the addition of relevant interventions and behaviors, such as use of pesticides and biological methods, use of repellants, wearing protective clothing, and reduction of mosquito breeding sites.

### Acknowledgements

This research used resources provided by the Los Alamos National Laboratory Institutional Computing Program, which is supported by the U.S. Department of Energy National Nuclear Security Administration. This research has been supported by the National Science Foundation (NSF) Science, Engineering, and Education for Sustainability (SEES)

grant CHE-1314029. This research has been supported by grants U01-GM097658-01 and U01-GM097661 from the NIH/NIGMS Models of Infectious Disease Agent Study (MIDAS) program. This research has been supported at Los Alamos National Laboratory under the Department of Energy contract DE-AC52-06NA25396.

## REFERENCES

- [1] Adams, B., Kapan, D.D., 2009, "Man bites mosquito: understanding the contribution of human movement to vector-borne disease dynamics." *PloS one* vol. 4 no. 8 pp. e6763.
- [2] Anyamba, A., Linthicum, K.J., Small, J.L., 2012, "Climate teleconnections and recent patterns of human and animal disease outbreaks." *PLoS Neglected Tropical Diseases* vol. 6 no. 1 pp. e1465.
- [3] Åström, C., Rocklöv, J., Hales, S., et al., 2013, "Potential distribution of dengue fever under scenarios of climate change and economic development." *EcoHealth* 1–7.
- [4] Bacaër, N., 2007, "Approximation of the basic reproduction number  $R_0$  for vector-borne diseases with a periodic vector population." *Bulletin of Mathematical Biology* vol. 69 no. 3 pp. 1067–1091.
- [5] Bouden, M., Moulin, B., Gusselin, P., "Epidemic propagation of west nile virus using a multi-agent geo-simulation under various short-term climate scenarios." *Proceedings of the 2008 Spring Simulation Multiconference (SpringSim'08)* pp. 98–105.
- [6] Chao, D.L., Halstead, S.B., Halloran, M.E., et al., 2012, "Controlling dengue with vaccines in Thailand." *PLoS Neglected Tropical Diseases* vol. 6 no. 10 pp. e1876.
- [7] Chao, D.L., Longini Jr, I.M., Halloran, M.E., 2013, "The effects of vector movement and distribution in a mathematical model of dengue transmission." *PloS one* vol. 8 no. 10 pp. e76044.
- [8] Chitnis, N., Hyman, J.M., Manore, C.A., 2013, "Modelling vertical transmission in vector-borne diseases with applications to Rift Valley fever." *Journal of biological dynamics* vol. 7 pp. 11–40.
- [9] Curtis, A., 2008, "Three-dimensional visualization of cultural clusters in the 1878 yellow fever epidemic of New Orleans." *International Journal of Health Geographics* vol. 7 no. 1.
- [10] Dumont, Y., Chiroleu, F., 2010, "Vector control for the Chikungunya disease." *Mathematical Biosciences and Engineering* vol. 7 no. 2 pp. 315–348.
- [11] Dumont, Y., Chiroleu, F., Domerg, C., 2008, "On a temporal model for the Chikungunya disease: Modeling, theory and numerics." *Mathematical Biosciences* vol. 213 no. 1 pp. 80–91.
- [12] D3js, 2013 D3.js - Data Driven Documents. <http://d3js.org/> Accessed 10 February 2014
- [13] Esteva, L., Vargas, C., 1998, "Analysis of a dengue disease transmission model." *Mathematical Biosciences* vol. 150 no. 2 pp. 131–151.

- [14] Guzman, A., Istúriz, R.E., 2010, "Update on the global spread of dengue." *International Journal of Antimicrobial Agents*, vol. 36 pp. S40–S42.
- [15] LaDeau, S.L., Leisnham, P.T., Biehler, D., et al., 2013, "Higher mosquito production in low-income neighborhoods of Baltimore and Washington, DC: understanding ecological drivers and mosquito-borne disease risk in temperate cities." *Int J Environ Res Public Health* 10(4): pp. 1505–1526.
- [16] Leaflet, 2010, Leaflet. <http://leafletjs.com/> Accessed 10 February 2014
- [17] Maciejewski, R., Rudolph, S., Hafen, R., 2010, "A visual analytics approach to understanding spatiotemporal hotspots." *IEEE Transactions on Visualization and Computer Graphics* vol. 16 No. 2 pp. 205–220.
- [18] Mackenzie, D., 2013, "Threatwatch: chikungunya virus spreads in the Americas." *New Scientist* vol. 220 no. 2948 pp. 10.
- [19] Manore, C.A., Hickmann, K.S., Hyman, J.M., et al., 2014, "A network-patch methodology for adapting agent-based models for directly transmitted disease to vector-borne disease." <http://arxiv.org/abs/1405.2258>
- [20] Manore, C.A., Hickmann, K.S., Xu, S., et al., 2014, "Comparing dengue and chikungunya emergence and endemic transmission in *A. aegypti* and *A. albopictus*." *Journal of Theoretical Biology* no. 0. <http://www.sciencedirect.com/science/article/pii/S002251931400263X>
- [21] Michaels, J., 2003, "Commercial buildings energy consumption survey." [http://www.eia.doe.gov/emeu/cbecs/cbecs2003/detailed\\_tables\\_2003/detailed\\_tables\\_2003.html](http://www.eia.doe.gov/emeu/cbecs/cbecs2003/detailed_tables_2003/detailed_tables_2003.html) Accessed 10 February 2014
- [22] Mniszewski, S.M., Del Valle, S.Y., Stroud, P.D., et al., 2008, "Pandemic simulation of antivirals + school closures: buying time until strain-specific vaccine is available." *Comput Math Organ Theory* 2008 14:209–221.
- [23] Mniszewski, S.M., Del Valle, S.Y., Stroud, P.D., et al., 2008, "EpiSimS simulation of a multi-component strategy for pandemic influenza." *Proceedings of the 2008 Spring Simulation Multiconference (SpringSim'08)* pp. 556–563.
- [24] Moulay, D., Aziz-Alaoui, M.A., Cadivel, M., 2011, "The chikungunya disease: modeling, vector and transmission global dynamics." *Mathematical Biosciences* vol. 229 no. 1 pp. 50–63.
- [25] Moulay, D., Aziz-Alaoui, M.A., Kwon, H., 2012, "Optimal control of chikungunya disease: larvae reduction, treatment and prevention." *Mathematical Biosciences and Engineering* vol. 9 no. 2 pp. 369–392.
- [26] Perkins, T.A., Scott, T.W., Le Menach, A., et al., 2013, "Heterogeneity, mixing, and the spatial scales of mosquito-borne pathogen transmission." *PLoS computational biology* vol. 9 no. 12 pp. e1003327.
- [27] Poletti, P., Messeri, G., Ajelli, M., et al., 2011, "Transmission potential of chikungunya virus and control measures: the case of Italy." *PLoS One*, vol. 6, no. 5, pp. e18860.
- [28] Press, W.H., Vetterling, W.T., Flannery, B.P., et al., 2007, *Numerical recipes 3rd edition: the art of scientific computing*. Cambridge University Press.
- [29] Reiner Jr, R.C., Stoddard, S.T., Scott, T.W., 2014, "Socially structured human movement shapes dengue transmission despite the diffusive effect of mosquito dispersal." *Epidemics* No. 0. <http://www.sciencedirect.com/science/article/pii/S1755436513000558>.
- [30] Robinson, M.C., 1955, "An epidemic of virus disease in Southern Province, Tanganyika Territory, in 1952–53." *Transactions of the Royal Society of Tropical Medicine and Hygiene* vol. 49 no. 1 pp. 28–32.
- [31] Silverman, B.W., 1986, "Density Estimation for Statistics and Data Analysis." *Monographs on Statistics and Applied Probability*.
- [32] Stoddard, S.T., Forshey, B.M., Morrison, A.C., et al., 2013, "House-to-house human movement drives dengue virus transmission." *Proceedings of the National Academy of Sciences*, vol. 110 no. 3 pp. 994–999.
- [33] Stroud, P., Del Valle, S., Sydoriak, S., et al., 2007, "Spatial dynamics of pandemic influenza in a massive artificial society." *JASSS* 10;4 9.
- [34] Thiboutot, M.M., Kannan, S., Kawalekar, O.U., 2010, "Chikungunya: a potentially emerging epidemic?" *PLoS Neglected Tropical Diseases* vol. 4 no. 4.
- [35] U.S. Department of Transportation (DOT), 2003, Bureau of transportation statistics NHTS 2001 highlights report BTS03-05.
- [36] Vanwambeke, S.O., Bennett, S.N., Kapan, D.D., 2011, "Spatially disaggregated disease transmission risk: land cover, land use and risk of dengue transmission on the island of Oahu." *Tropical Medicine & International Health* vol. 16 no. 2 pp. 174–185.
- [37] Wearing, H.J., Rohani, P., 2006, "Ecological and immunological determinants of dengue epidemics." *Proceedings of the National Academy of Sciences* vol. 103 no. 31 pp. 11802–11807.
- [38] Yakob, L., Clements, A. CA, 2013, "A mathematical model of chikungunya dynamics and control: the major epidemic on Réunion Island." *PLoS One* vol. 8 no. 3 pp. e57448.
- [39] Yee, D., Bradford, J., 1999, "Employment density study." Canadian METRO Council Technical Report.
- [40] Yu, H., Christakos, G., 2006, "Spatiotemporal Modelling and mapping of the bubonic plague epidemic in India." *International Journal of Health Geographics* vol. 5 no. 1.
- [41] Zhou, Y., Niaz Arifin, S.M., Gentle, J., Kurtz, S.J., Davis, G.J., Wendelberger, B.A., 2010, "An agent-based model of the anopheles gambiae mosquito life cycle." *Proceedings of the 2010 Summer Computer Simulation Conference (SCSC'10)* pp. 201–208.